US005749542A

United States Patent [19]

Hamstra et al.

[11] **Patent Number: 5,749,542**

[45] **Date of Patent: May 12, 1998**

[54] **TRANSITION SHOULDER SYSTEM AND METHOD FOR DIVERTING BOUNDARY LAYER AIR**

[75] Inventors: **Jeffrey William Hamstra**, Fort Worth; **Brent Neal McCallum**, Benbrook; **Thomas Gerard Sylvester**; **Brett Willian Denner**, both of Fort Worth; **Jeffrey Allen Moorehouse**, Arlington, all of Tex.

[73] Assignee: **Lockheed Martin Corporation**, Fort Worth, Tex.

[21] Appl. No.: **654,295**

[22] Filed: **May 28, 1996**

[51] **Int. Cl.**^{6} **B64D 33/02**

[52] **U.S. Cl.** .... **244/53 B**; 137/15.1

[58] **Field of Search** .... 244/53 R, 53 B, 244/74, 204; 137/15.1, 15.2

[56] **References Cited**

U.S. PATENT DOCUMENTS

3,066,892	12/1962	Smith et al.	244/53 B
3,137,460	6/1964	Owl, Jr. et al.	244/53 B
3,667,704	6/1972	Assmann	137/15.1
4,502,651	3/1985	Jungclaus et al.	244/53 B
4,655,413	4/1987	Genssler et al.	137/15.1

Primary Examiner—Galen L. Barefoot

Attorney, Agent, or Firm—Baker & Botts, L.L.P.

[57] **ABSTRACT**

A diverterless engine inlet system that integrates a transition shoulder into a system for diverting air from the inlet of an aircraft engine. ????? The bump includes an isentropic compression surface raised outwardly from the body of the aircraft to form a portion of the inner surface of the inlet. The transition surface works with the compression surface to divert low energy boundary layer air from the inlet during aircraft operation.

28 Claims, 10 Drawing Sheets

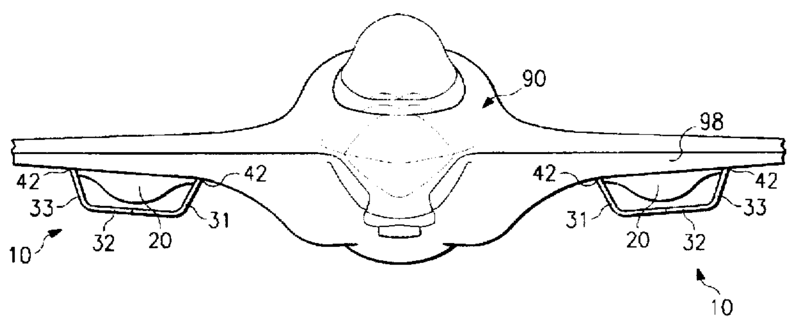

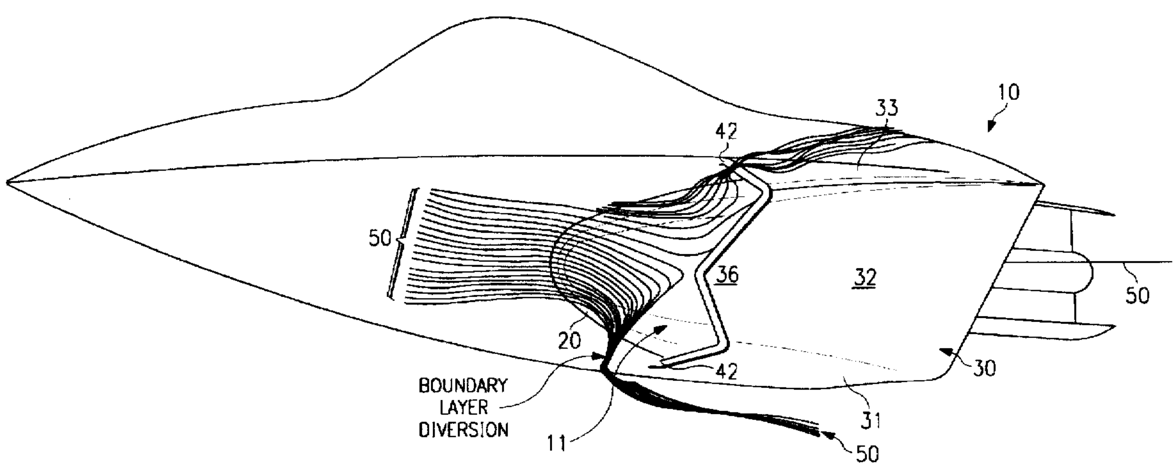

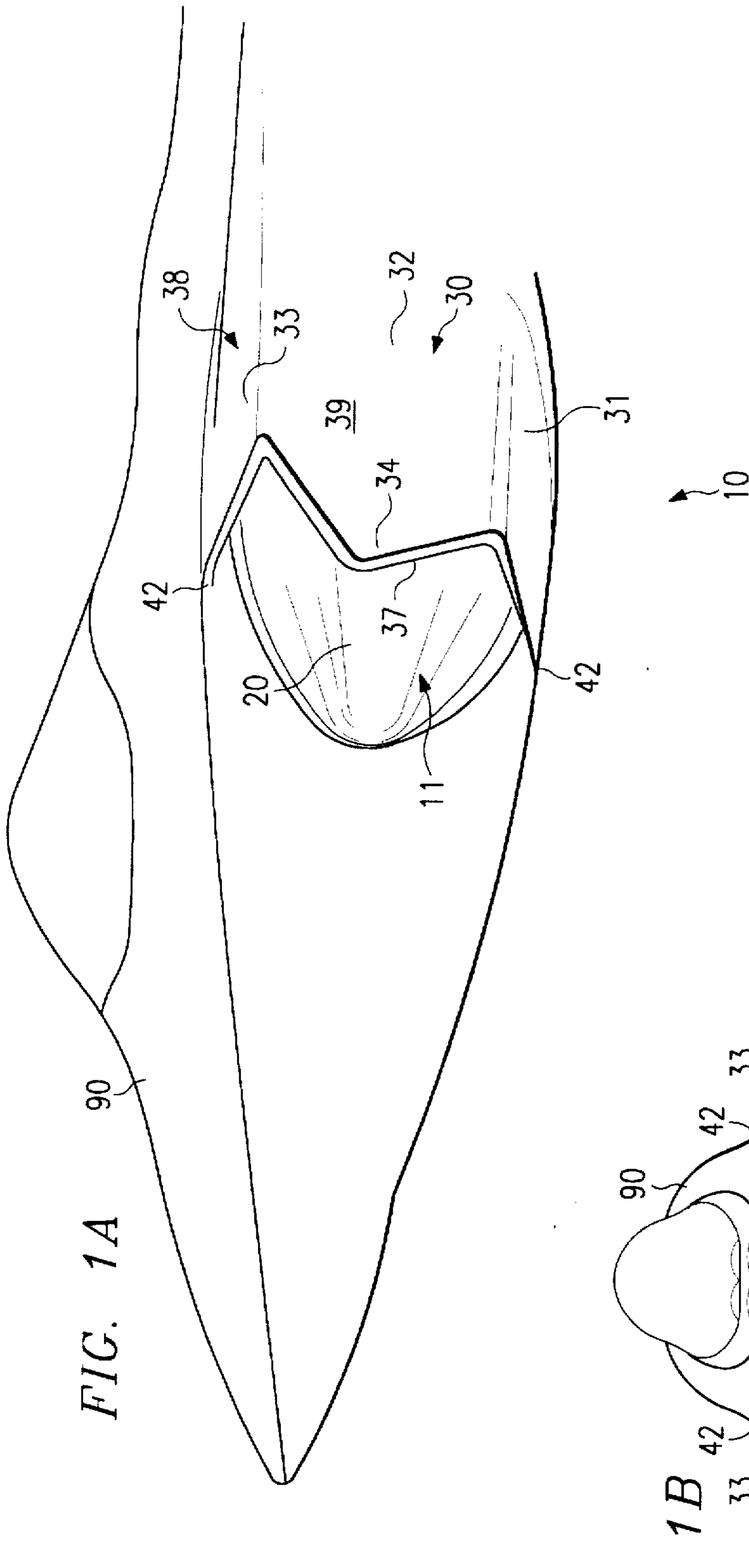
38
33
33
32
30
39
31
34
42
37
20
42
11
10
90

FIG. 1A

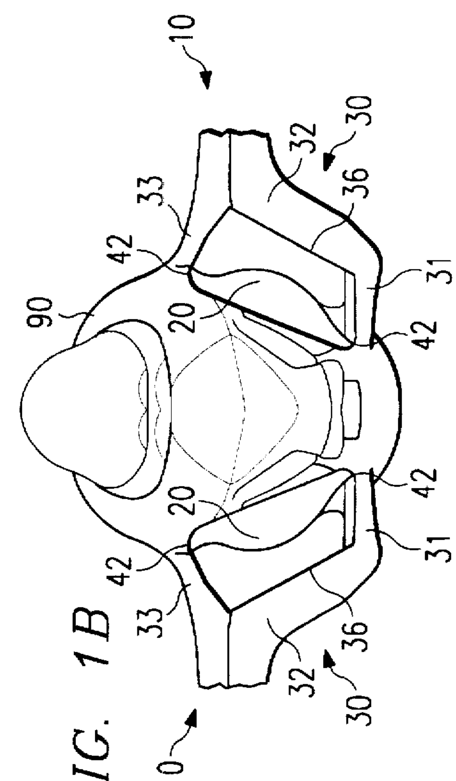
10
30
32
36
33
42
31
90
20
42
42
20
31
42
33
36
32
30
10

FIG. 1B

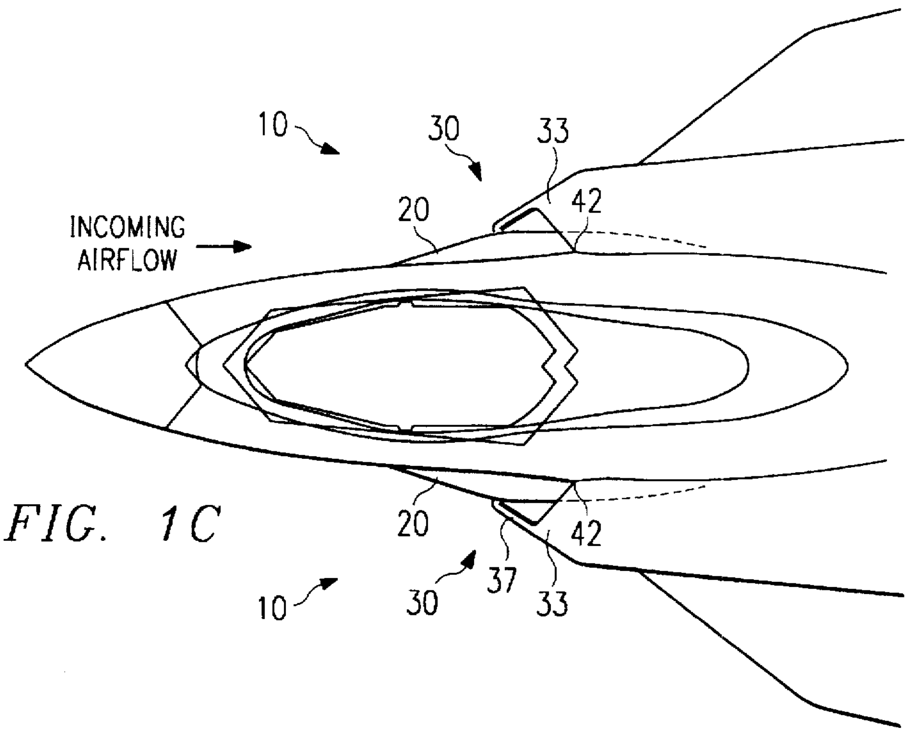

FIG. 1C

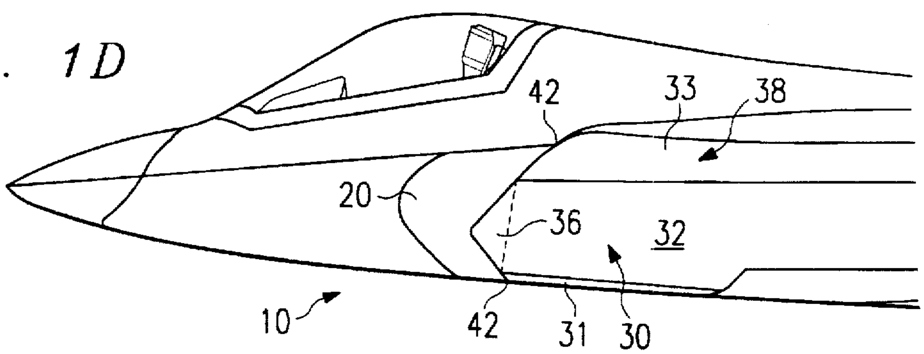

FIG. 1D

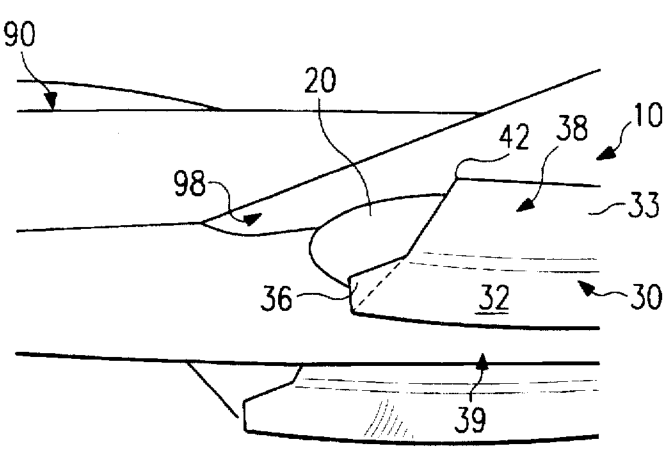

FIG. 2A

FIG. 2B

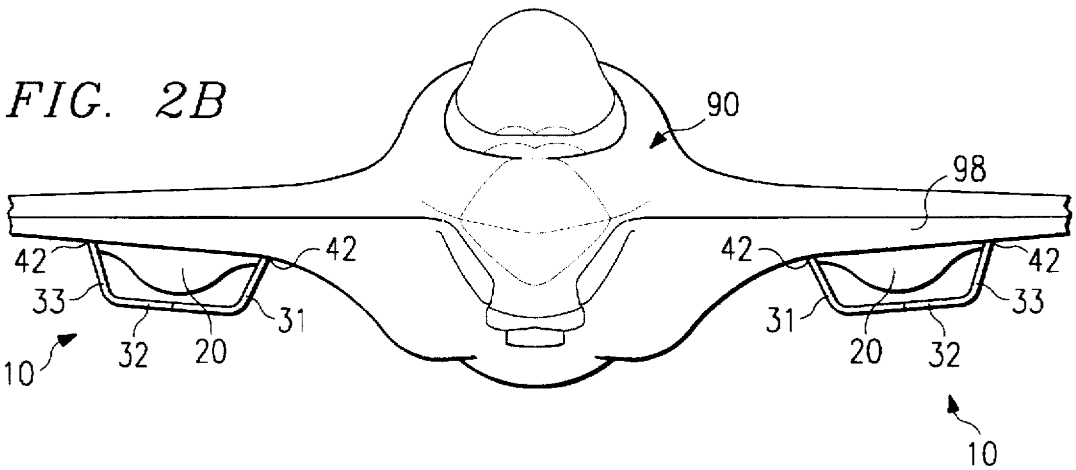

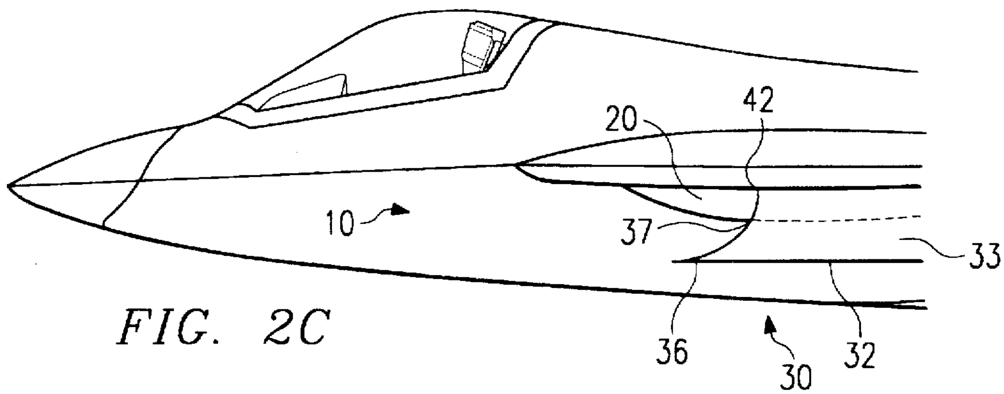

FIG. 2C

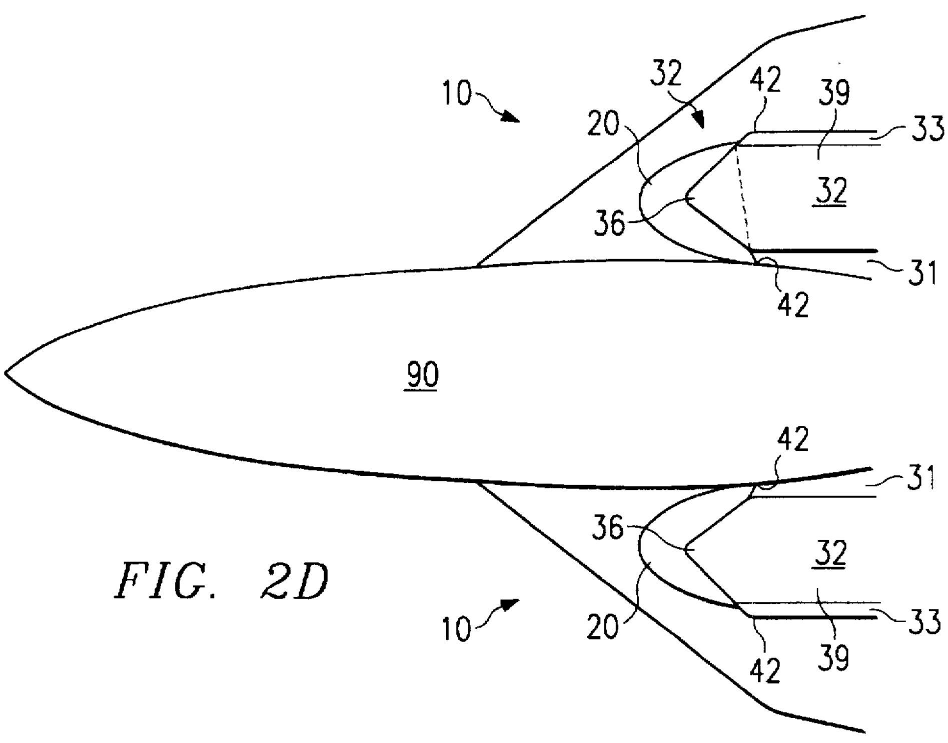

FIG. 2D

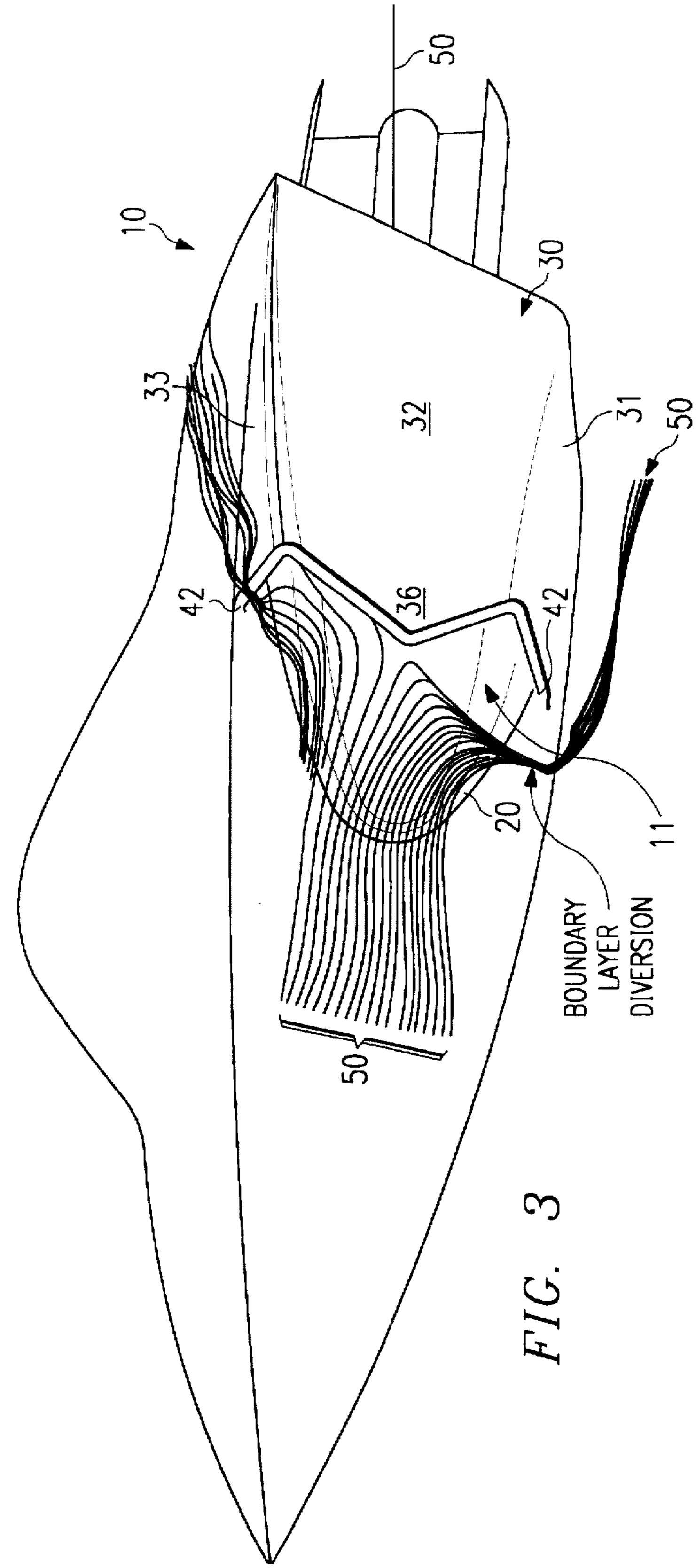

FIG. 3

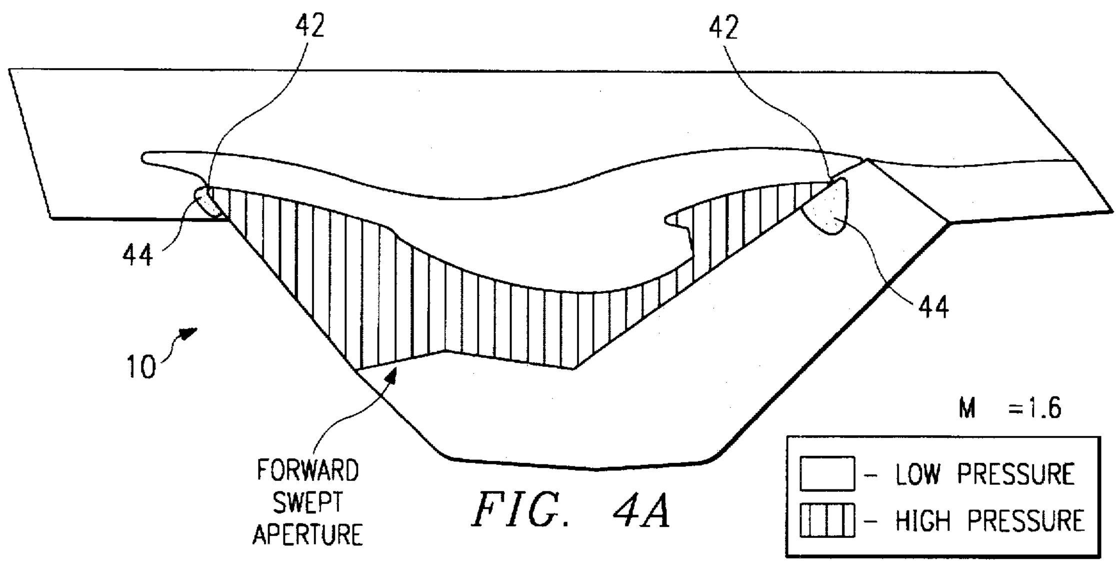
42
42
44
44
10
M =1.6
FORWARD
SWEPT
APERTURE
- LOW PRESSURE
- HIGH PRESSURE

FIG. 4A

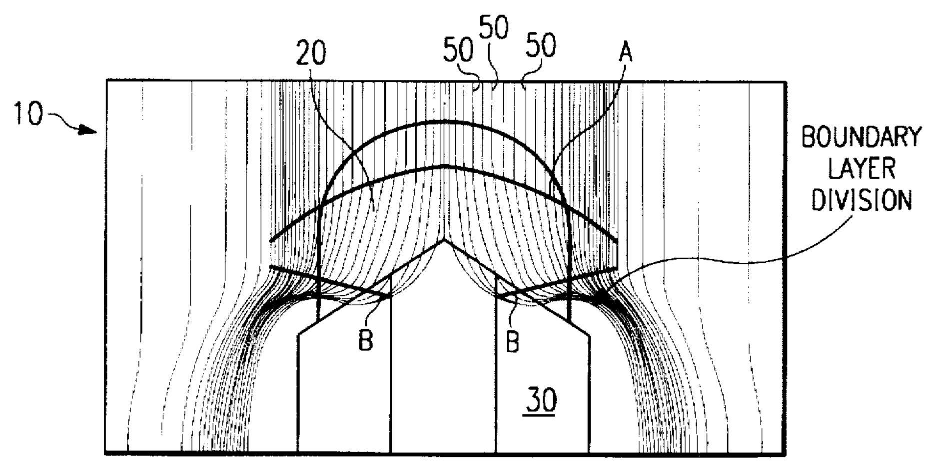
20
50
50
50
A
10
BOUNDARY
LAYER
DIVISION
B
B
30

FIG. 4B

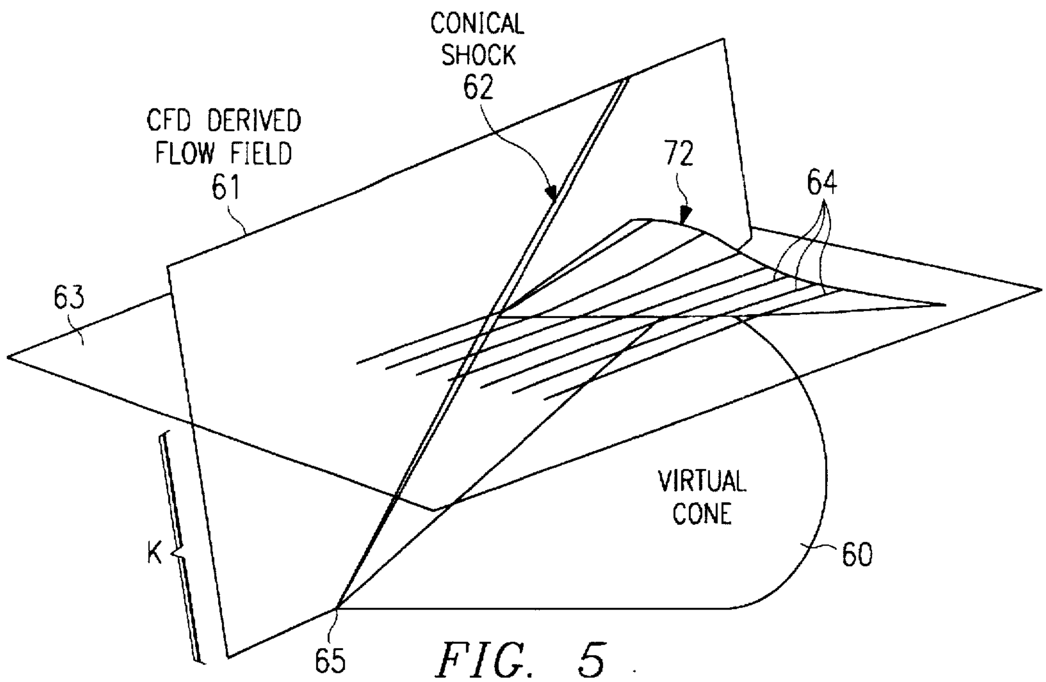

FIG. 5

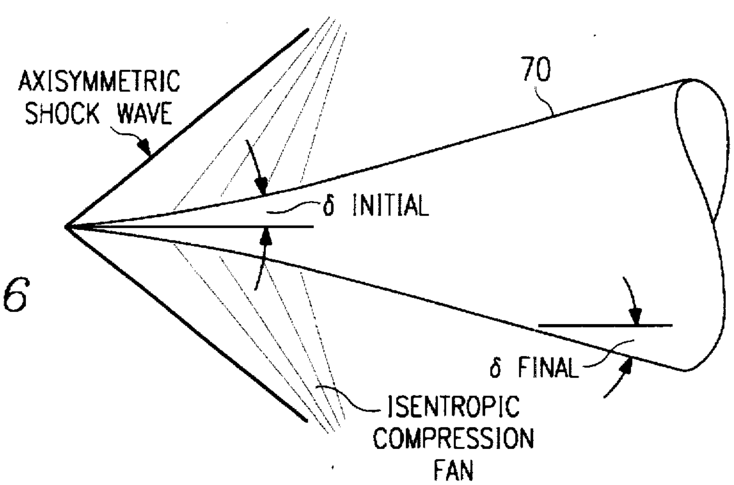

FIG. 6

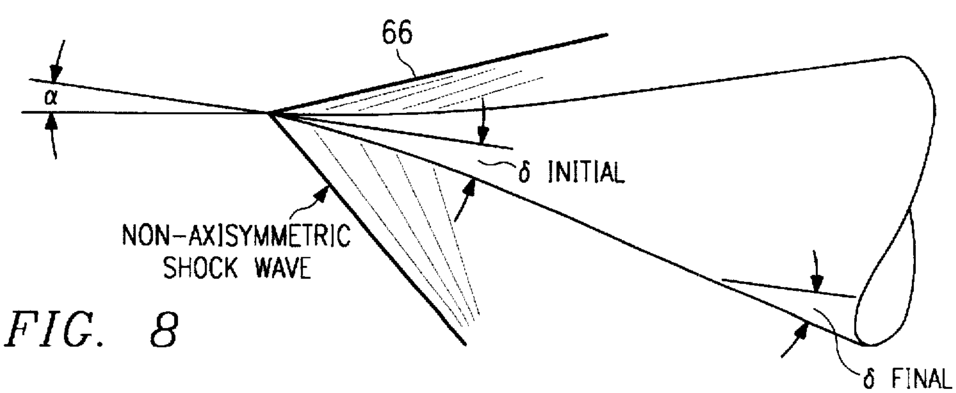

FIG. 8

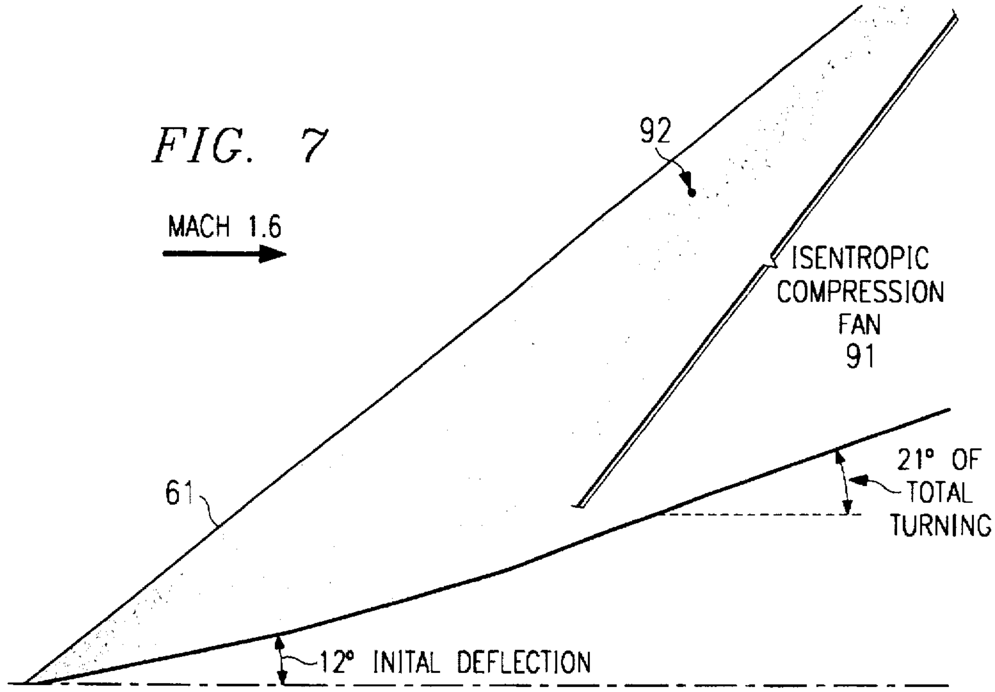
92
MACH 1.6
ISENTROPIC
COMPRESSION
FAN
91
21° OF
TOTAL
TURNING
61
12° INITAL DEFLECTION

FIG. 7

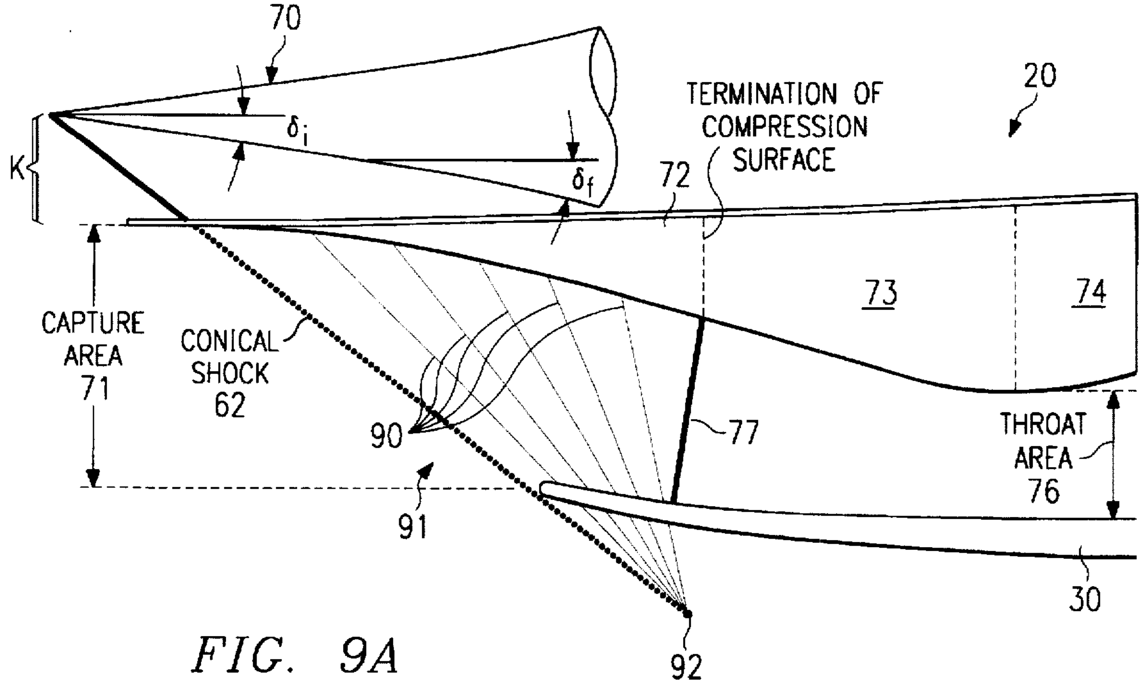
ISENTROPIC
CONE
70
TERMINATION OF
COMPRESSION
SURFACE
20
δ_i
δ_f
72
K
73
74
CAPTURE
AREA
71
CONICAL
SHOCK
62
90
77
THROAT
AREA
76
91
30
92

FIG. 9A

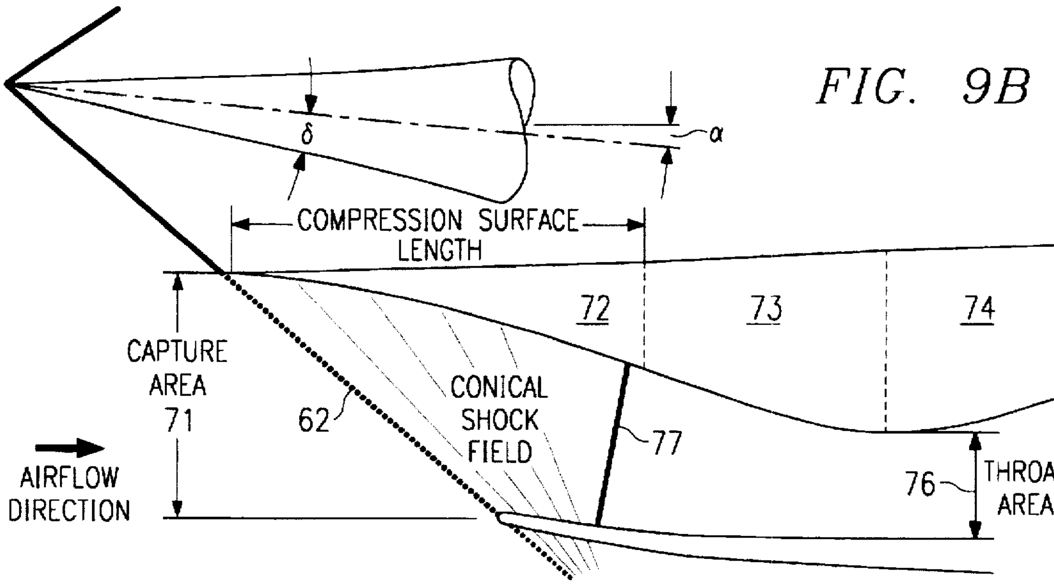

FIG. 9B

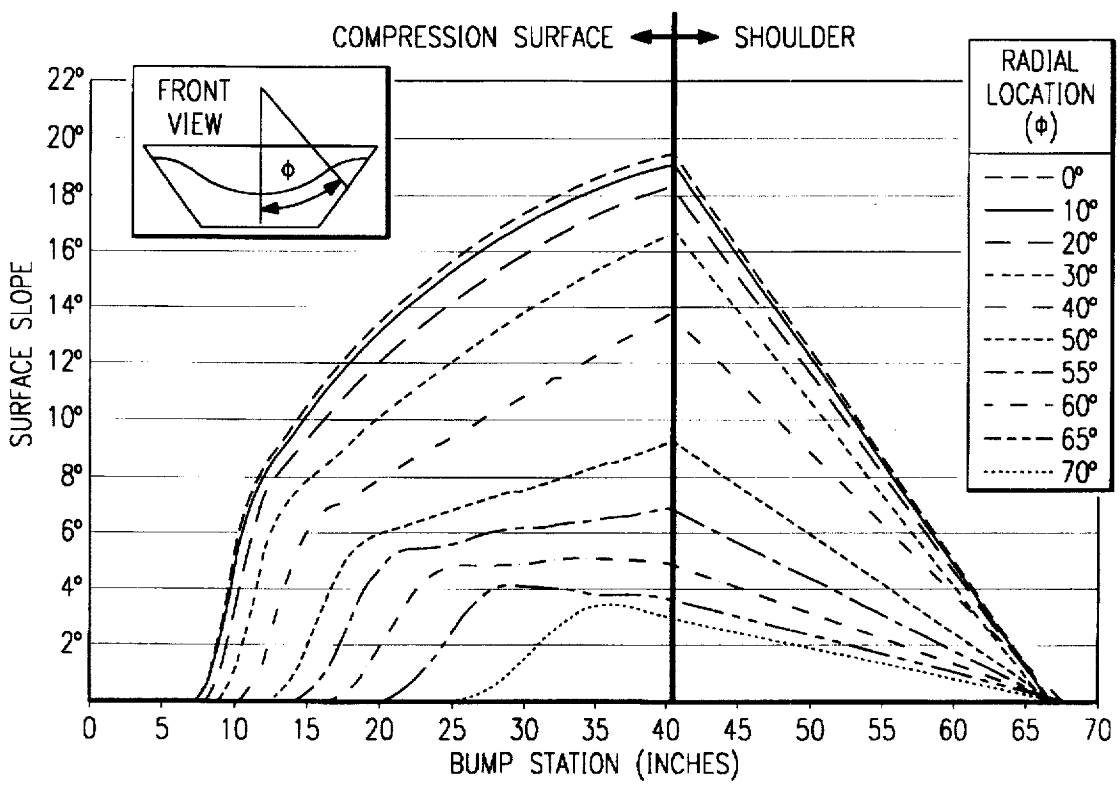

FIG. 10A

FIG. 10B

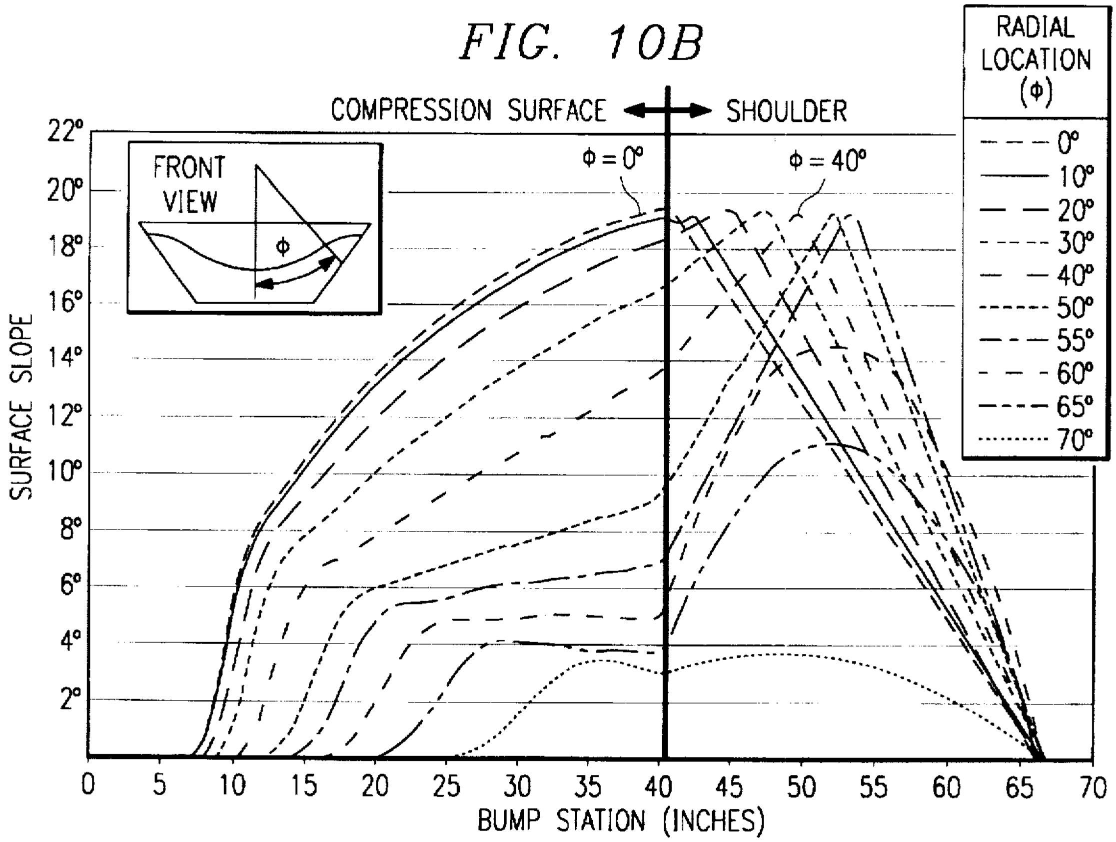

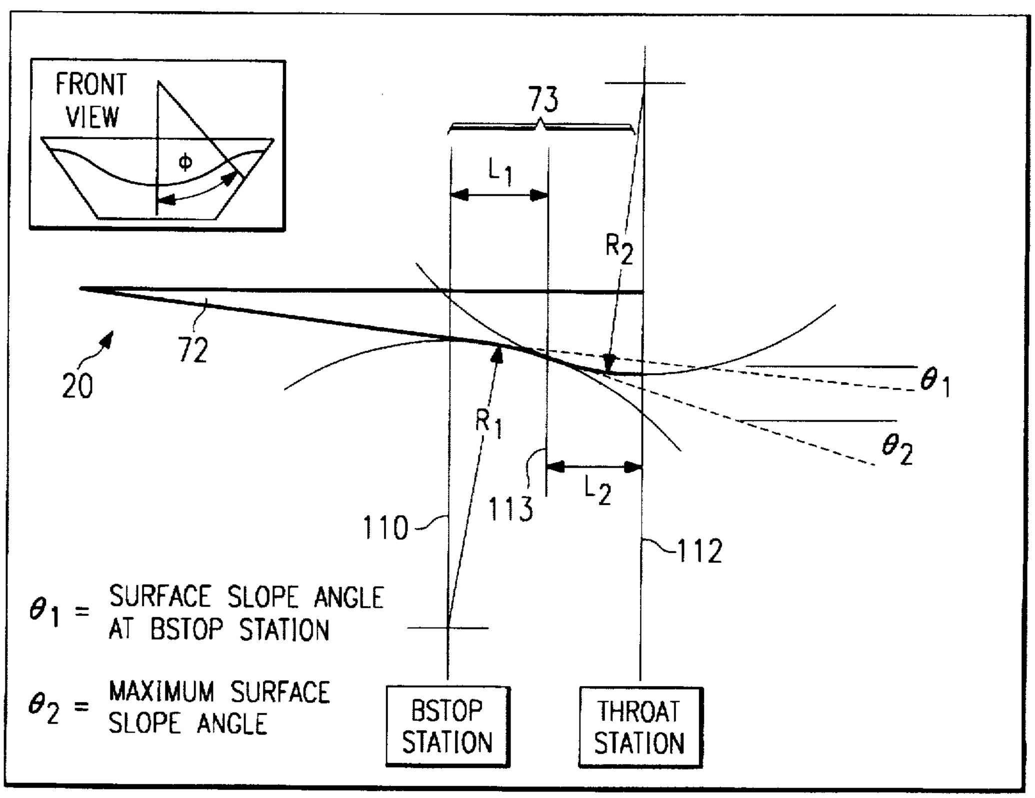

FIG. 11

FIG. 12

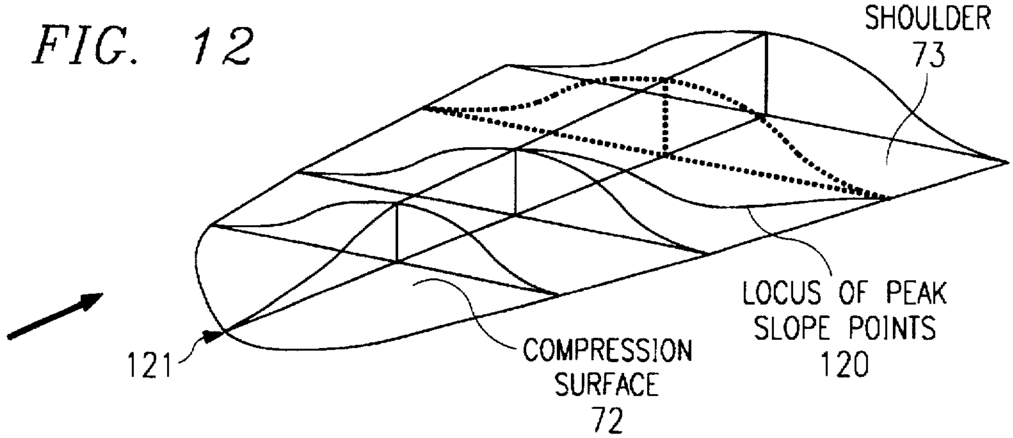

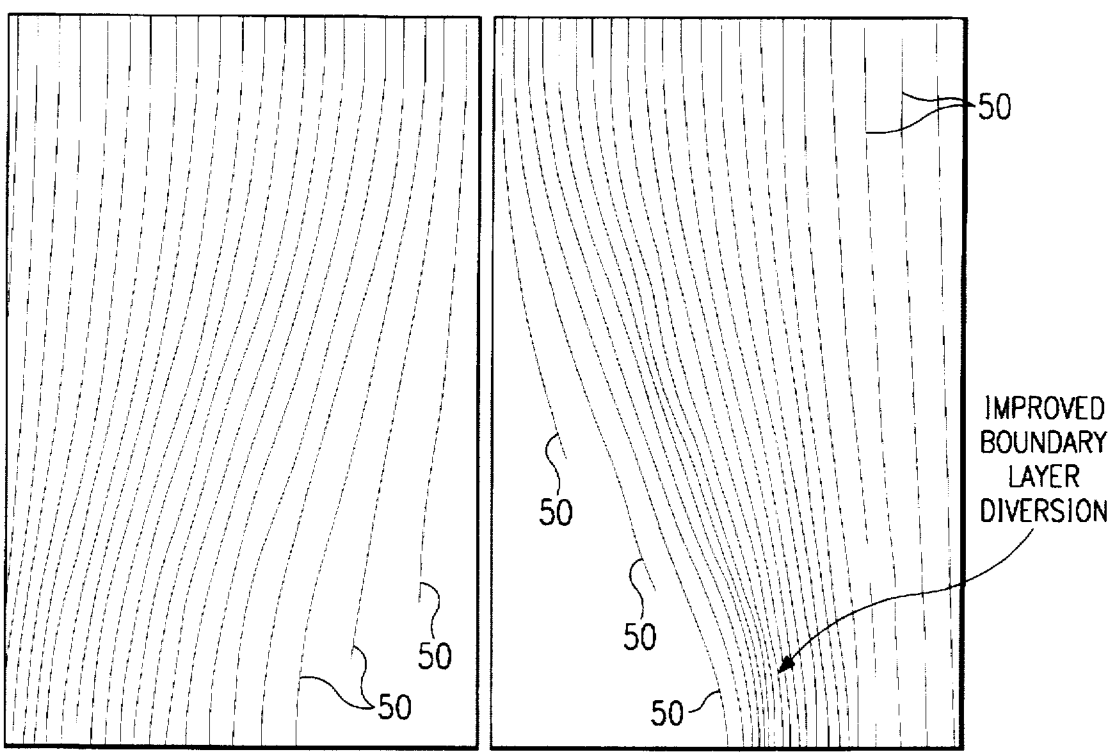

FIG. 13A FIG. 13B

TRANSITION SHOULDER SYSTEM AND METHOD FOR DIVERTING BOUNDARY LAYER AIR

TECHNICAL FIELD OF THE INVENTION

The present invention relates in general to engine inlet systems, and more particularly, to a transition shoulder system and method for diverting boundary layer air from the inlet of an engine.

BACKGROUND OF THE INVENTION

Many of today's fighter aircraft must cruise supersonic while maintaining low radar cross-sections to avoid detection on radar. The engine inlets on the aircraft must also work well supersonically while having a low radar cross-section.

During high speed flight, a very low velocity, low pressure boundary layer of air builds up on the fuselage of a supersonic aircraft. Because this low energy air can cause poor engine performance, high speed aircraft have traditionally employed some type of boundary layer diverter system to prevent the boundary layer air from entering the inlet. Current advanced supersonic tactical aircraft utilize air induction systems that include boundary layer diverters, boundary layer bleed systems, and overboard bypass systems to divert this boundary layer air in order to provide higher engine inlet performance.

A boundary layer diverter is essentially a gap between the side of the aircraft body and the inlet that diverts the low-pressure boundary layer air that builds up on the fuselage and prevents this boundary layer air from entering the engine. In addition to the diverter, traditional inlet systems also utilize a boundary layer bleed system on the edge of the inlet. The bleed system works in a manner similar to the diverter, except instead of skimming off the boundary layer air, the bleed system takes that air on-board, then vents it up through the airplane and exhausts it through a bleed exit on the aircraft. In addition to a diverter and a bleed system, some traditional inlet systems also use an overboard bypass system The bypass system exists to correct a high speed problem with the aerodynamics of traditional inlet systems. The inlet has to flow a certain amount of air to work properly. At high speeds, the engine airflow demand cuts back to a level below that required for the inlet to work properly. The bypass system compensates by dumping the excess air overboard.

Present air induction systems require these subsystems in order to make this low observable inlet design work properly at high speeds. These systems are highly complex and involve a variety of composite materials. These air induction systems increase the weight, the cost of production, mechanical complexity and the cost of maintenance of the aircraft.

The "bump" concept of having a raised compression surface has been discussed in industry references, most recently in a book entitled "Intake Aerodynamics," edited by J. Seddon and E. L. Goldsmith, and published in 1985 by the American Institute of Aeronautics and Astronautics. Performance of an inlet with a compression surface was measured and documented in the 1956 report "Performance of External-Compression Bump Inlet at Mach Numbers of 1.5 to 2.0," by Simon, Brown, and Huff (NACA RM E56119). However, the concept reported therein, unlike the present invention, utilized an unswept cowl and bump surface boundary layer bleed Bump inlet technology was also examined in the Air Force Wright Laboratory program "Management of Advanced Inlet Boundary Layers" (Contract F33615-89-C-3000). This program examined a bump inlet concept with a bleed system and a serrated cowl designed to optimize, rather than eliminate, boundary layer diverters and bleed systems.

SUMMARY OF THE INVENTION

In accordance with the present invention, a system and method for diverting boundary layer air from an aircraft engine is provided that substantially eliminates or reduces disadvantages and problems associated with previously developed engine inlet systems.

The present invention provides a diverterless inlet system that uniquely integrates a "bump" including an isentropic compression surface with a forward swept, aft-closing cowl. The bump is a surface raised outwardly from the body of the aircraft. The cowl couples to the body of the aircraft and forms the outer surfaces of the inlet. The cowl closes against the body of the aircraft at the aft-most points of the inlet opening. The bump and the cowl work together to divert boundary layer air and prevent substantially all of the lower energy boundary layer air from flowing through the inlet during aircraft operation.

A technical advantage of the present invention is that the forward-swept, aft-closing cowl and the isentropic compression surface reduce the complexity of the aircraft's inlet system. In particular, the present invention does not require a boundary layer diverter, a side or splitter plate, a boundary layer bleed system, or an overboard bypass system. Furthermore, the present invention has no moving parts. This reduction in complexity reduces the tactical fighter aircraft's empty weight, production cost, and maintenance support requirements. These savings are estimated to be 250 pounds per aircraft, $225,000 per aircraft, and 0.03 maintenance man hours per flight hour, respectively.

The present invention provides another technical advantage in that it is adaptable to virtually any supersonic aircraft.

Because all inlet designs spill air from the inlet area, another technical advantage of the present invention is that it takes advantage of the fact that some air must be spilled outboard by spilling the lower quality boundary layer air, rather than the higher quality free stream air.

BRIEF DESCRIPTION OF THE DRAWINGS

For a more complete understanding of the present invention and the advantages thereof, reference is now made to the following description taken in conjunction with the accompanying drawings in which like reference numerals indicate like features and wherein:

FIG. 1A shows one embodiment of the present invention side-mounted to the body of an aircraft;

FIG. 1B illustrates a front view of a side-mounted embodiment of the present invention;

FIG. 1C illustrates a top view of a side-mounted embodiment of the present invention;

FIG. 1D illustrates a side view of a side-mounted embodiment of the present invention;

FIG. 2A shows another embodiment of the present invention mounted to the underside of a wing of an aircraft;

FIG. 2B illustrates a front view of a wing-mounted embodiment of the present invention;

FIG. 2C illustrates a side view of a wing-mounted embodiment of the present invention;

FIG. 2D illustrates a bottom view of a wing-mounted embodiment of the present invention;

FIG. 3 illustrates the one solution describing the boundary layer diversion associated with one embodiment of the present invention at Mach 1.6;

FIG. 4A illustrates an isometric view of the surface pressure coefficient of the same embodiment as shown in FIG. 4A of the present invention at Mach 1.6;

FIG. 4B illustrates a bottom view of the boundary layer diversion of the particle traces of another embodiment of the present invention at Mach 1.6;

FIG. 5 illustrates one derivation of the compression surface from a conical flow field;

FIG. 6 illustrates an isentropic cone for deriving a compression surface;

FIG. 7 illustrates one derivation of the isentropic compression surface at Mach 1.6;

FIG. 8 illustrates an isentropic cone presented at an angle of attack to the air flow for deriving a compression surface;

FIG. 9A shows another embodiment of the present invention utilizing an isentropic cone;

FIG. 9B shows another embodiment of the present invention utilizing an isentropic cone at an angle of attack;

FIG. 10A is a graphical representation of the surface slope of the compression surface and the transition shoulder;

FIG. 10B is a graphical representation of another embodiment of the compression surface and transition shoulder;

FIG. 11 illustrates the shape of one embodiment of the transition shoulder of the present invention;

FIG. 12 shows one embodiment of the compression surface and transition shoulder of the present invention; and

FIG. 13 illustrates graphically the diversion of boundary layer air outboard by two embodiments of the present invention

DETAILED DESCRIPTION OF THE INVENTION

The present invention provides a supersonic engine inlet concept for use in, for example, tactical aircraft applications, that utilizes a "bump" comprising a fixed three-dimensional, isentropic compression surface, a transition shoulder, and a diffuser fairing, combined with an aft-closing, forward-swept cowl which closes against the aircraft at the aft-most points of the inlet opening. The present invention eliminates the need for boundary layer diverters, overboard bypass systems, and boundary layer bleed systems currently used on conventional air induction systems for supersonic aircraft. Thus, the present invention reduces aircraft weight, cost, and complexity. These features are eliminated because the compression surface and cowl work synergistically to provide boundary layer diversion capability.

The compression surface portion of the bump, can be designed to produce a conical flow field that can be equivalent to that of an axisymmetric body with a 12° semivertex angle isentropically blended to a 21° final turning angle. The span-wise static pressure on the surface can begin to divert boundary layer air outboard. The pressure differential between the inlet and the area surrounding the inlet further diverts the boundary layer air outboard. The compression surface can also serve to reduce terminal shock Mach number, thus reducing the tendency for shock-induced flow separation. Because the cowl closes against the forebody at the aft-most points of the inlet opening, low pressure boundary layer air, rather than free stream air, can be diverted out the side of the inlet. The inlet concept of the present invention can be utilized in any number of forebody/aperture integration schemes.

FIG. 1A illustrates a side-mounted embodiment of the inlet **10** mounted to the body of an aircraft **90** with an opening **11** for receiving air into the inlet **10**. The inlet **10** includes a bump **20** and a forward-swept, aft-closing cowl **30**. The bump **20** is a raised surface formed outwardly from the aircraft towards the interior of the inlet **10**. The bump **20** forms part of the inner surface of the inlet **10**. The surface comprising the bump **20** begins to raise outwardly away from the body of the aircraft prior to the opening **11**, so that boundary layer air will contact the bump **20** prior to arriving at the opening **11**. The shape of the bump **20** can be varied depending on design parameters discussed more fully below.

As shown in FIG. 1B, this side-mounted embodiment of the bump **20** extends outwardly from the body of the aircraft **90** with highest point of the bump **20** approximately at the center of the inlet and the bump gradually lessens in height as it approaches the cowl **30**. FIG. 1C shows a side-mounted embodiment of the surface forming the bump **20** that gradually increase in height away from the body of the aircraft **90** near the opening **11**, reaches a peak at a point inside the inlet **10**, then gradually decreases in height near the rear of the inlet **10**.

The cowl **30** includes an aft-closing portion **38** and a forward-swept portion **39** shown generally in FIG. 1A. The embodiment of the aft-closing portion **38** shown in FIGS. 1B, 1C, and 1D includes a pair of aft-closing panel sections **31** and **33** that close against the body of the aircraft at the aft-most points **42** of the cowl. The embodiment of the forward-swept portion **39** shown in FIGS. 1B, 1C, and 1D includes forward-swept panel section **32** that further includes tip **36**. The forward-swept panel section **32** can include several sections joined together, or alternatively, can be a single piece. The embodiment of the cowl shown in FIG. 1A shows aft-closing panels **31** and **33** coupled to the body of the aircraft and extending outwardly from the aircraft. Aft-closing panels **31** and **33** include leading edge **37** that extends from the closure point **42** toward the front of the aircraft. Forward-swept panel section **32** joins aft-closing panel section **31** to aft-closing panel section **33** to form the cowl **30** that provides the outer frame of the inlet **10**. Coupling the cowl **30** to the body of the aircraft forms the opening **11** of the inlet **10**. The forward-swept panel section **32** of cowl **30** includes a triangular shaped tip **36** coming to a point at the forward-most point of the forward-swept panel section **32** to form the forward-swept portion **39** of the cowl. This side-mounted embodiment of the cowl **30** is also shown in FIGS. 1C and 1D. FIGS. 1C and 1D show the forward-swept portion **39** of the cowl **30** extending towards the front of the aircraft. FIG. 1D illustrates that the tip **36** of the forward-swept panel section **32** can be triangular in shape with an apex of the triangle approximately at the centerline of the inlet **10**. As shown in FIG. 1C, the aft-closing panel sections **31** and **33** can close against the body of the aircraft at closure points **42**. As illustrated in FIGS. 1C and 1D, cowl closure points **42** can be located at the aft-most points of the opening **11**. As illustrated in FIG. 1B, forward-swept panel section **32** can join aft-closing panel sections **31** and **33** to create a cowl **30** that forms an inlet opening **11** with an approximately trapezoid shape as the cowl **30** closes against the body of the aircraft.

FIG. 2A illustrates a wing-mounted embodiment of the inlet **10** with an opening **11** for receiving air into the inlet **10**. In this alternative embodiment, the raised surface of the bump **20** is formed outwardly from the bottom of the wing

98 of the aircraft 90. As before, the inlet 10 includes a bump 20 and a cowl 30. FIG. 2E, 2C and 2D show the front, side and bottom views respectively of the side-mounted embodiment of FIG. 2B. FIGS. 2A–D again illustrate an embodiment of the inlet 10 with an approximately trapezoidal shaped opening 11, an aft-closing, forward-swept cowl 30 with an approximately triangular tip 36 at the forward most part of the forward-swept panel section 32, and a bump 20 raised outwardly in a generally curved manner with a peak approximately on the centerline of the inlet 10. FIGS. 1A–D and 2A–D are by way of illustration and not limitation. For example, the panel sections 31, 32, and 33 that form the outer portion of the cowl 34 could be formed from a single piece. Furthermore, panel sections 31, 32, and 33 could be formed such that, when coupled to the body of the aircraft, the shape of the opening 11 was approximately elliptical. For further example, the tip 36 could be formed with a curved outer portion rather than the shape of a triangle.

In operation, the bump 20 and cowl 30 work together to divert substantially all of the boundary layer air from the inlet 10. As the aircraft moves, the boundary layer air flows toward the inlet 10 while remaining approximately near the aircraft surface. Prior to reaching the inlet opening 11, the boundary layer air contacts the bump 20 which alters boundary layer air's path of motion to begin diverting this air away from the inlet opening 11. The shape of the cowl 30 helps to establish a pressure differential so that the pressure near the inlet opening 11 and inside the inlet 10 is higher than the pressure outside the opening 11. The shape of the cowl 30 creates a significantly lower pressure at the closure points 42. Thus, once the boundary layer air begins moving outboard due to the bump 20, the boundary layer air moves to the lower pressure regions near the closure points 42 and outside the inlet 10, rather than the higher pressure regions near the opening 11 of the inlet 10. This pressure gradient continues to divert boundary layer air during operation of the aircraft.

Computer programs generate an image of an aircraft using computational fluid dynamics (CFD) analysis and aerodynamic simulation to model this inlet design. The computer program illustrates what the pressure field looks like around the inlet 10 and where the air flows in and around the inlet 10. FIG. 3 represents a solution of the present invention at Mach 1.6 for a side-mounted inlet 10. As indicated above, the interior of the inlet 10 and near the opening 11 are at a higher pressure region relative to the exterior of the cowl 30 and the closure points 42. The lines represent the paths 50 that particles or elements of boundary layer air travel. The paths 50 show how the bump 20 and cowl 30 work together to divert this boundary layer overboard. As the particles in the paths 50 approach the inlet 10, the bump 20 starts subtly moving the boundary layer air outboard. As shown by the paths 50, the boundary layer air particles then take a more extreme turn and go toward the outer edges of the cowl 30 due to the high pressure in the inlet 11 area that forces the boundary layer air to spill out to a lower pressure region. The higher pressure diverts the lower pressure, lower velocity boundary layer out around the cowl 30 and prevents substantially all of this lower energy boundary layer air from entering the inlet 10.

The inlet concept of the present invention will divert boundary layer air just by using the cowl 30 concept. However, the present invention without the bump 20 will only divert boundary layer to a certain Mach level. In order to divert substantially all of the boundary layer air at Mach 1.6 or higher, the present invention must utilize both the bump 20 and the cowl 30.

FIG. 4A shows a CFD analysis on another embodiment of the present invention. In FIG. 4A, the surface pressure of the inlet 10 area is coded in terms of pressure contour where the dotted areas indicate lower pressure regions and cross-hatched areas represent regions of higher pressure. The areas marked 44 near the closure points 42 represent the lowest pressure region areas. FIG. 4A demonstrates that, in operation, the interior of the inlet 10 is at a higher pressure relative to the exterior of the cowl 30. FIG. 4B shows that as the particle trace paths 50 of the boundary layer air approach the bump 20, a subtle deflection of the particles outboard occurs as shown at point A. Due to the higher pressure region in the inlet 10, the boundary layer air particles then take a more extreme turn at point B and are diverted toward the outer edges and the closure points 42 of the cowl 30. As illustrated in FIG. 4B, the bump 20 causes the boundary layer air to start moving outboard and the higher pressure forces the boundary layer air to take a more extreme turn towards the outer edges of the cowl 30.

As shown in FIG. 9A, the bump 20 comprises a compression surface 72, a transition shoulder 73, and a diffuser fairing 74. The shape of the compression surface 72 of the bump 20 can be determined by CFD computerized analysis. As illustrated in FIG. 5, in a computerized model, placing a virtual right circular cone 60 with a constant semi-vertex angle in a supersonic CFD derived flow field 61 will create a conical shock 62 field that is axisymmetric around the virtual cone 60 emanating from the apex 65 of the virtual cone 60. A plane of particles 63 is released and sent through the axisymmetric conical shock 62 at a distance above the apex of the cone known as k. The width of the cone formed by the conical shock 62 at the intersections of the conical shock cone with the plane of particles 63 is denoted as w. The ratio of k to w (k/w) is approximately 0.1 for the embodiment shown in FIG. 5. The particles 64 in the plane of particle released 63 propagate into the flow field and will alter course as the particles 64 pass through the conical shock 62. The shape formed above the original plane of release 63 after passing through the conical shock 62 defines the shape of a compression surface 72 that can be applied to the surface of the aircraft. If a compression surface 72 formed from this procedure is placed in the same flow field, the particles will flow as shown in FIG. 5. A computer program could store this compression surface 72 in its memory and apply the necessary contour of the compression surface 72 to the given shape of the aircraft. The computer must contain a definition of the flow field generated by the virtual cone and a definition of the particle release plane 63, then the computer program can generate the compression surface.

In an alternative embodiment, a parabolic shape, an elliptical shape, or a wedge could be used, rather than a right circular cone, to produce a flow field that could generate a compression surface 72.

FIG. 6 illustrates that an isentropic cone 70, rather than a right circular virtual cone 60 with a constant semi-vertex angle, can be used to create an isentropic compression surface 72. The isentropic cone 70 is used in the same manner described above to produce a flow field through which a plane of particles is released to determine the shape of the compression surface 72. The isentropic cone 70 has a cross section defined by an initial semi-vertex angle δ_i relative to the centerline of the isentropic cone 70 and a final vertex angle δ_f relative to the centerline of the isentropic cone 70. As shown in FIG. 6, the isentropic cone 70 has a smaller initial semi-vertex angle that gradually increases to a larger final vertex angle. The embodiment of FIG. 7 shows an the isentropic cone **70** with a lower semi-vertex angle defined by a deflection angle of 12° that gradually increases to reach a final vertex angle with a final deflection angle of 210°. These initial and final deflection angles are illustrative and can be modified to achieve a total turning angle of approximately 21 degrees.

FIG. **8** shows yet another embodiment of the virtual cone used to define the shape of the bump **20** where the isentropic cone **70** has been positioned relative to the release of particles **63** so that the centerline of the isentropic cone **70** is offset from the airflow release plane of particles **63** by an angle of attack α. Positioning a virtual cone at an angle of attack α relative to a computer generated supersonic CFD derived flow field **61** will create a non-axisymmetric (or distorted) conical shock **66** wave emanating from the apex of the virtual cone. Whereas an axisymmetric conical shock wave **62** has a circular cross section, the non-axisymmetric shock wave **66** will have an elliptical cross section. The angle of attack α illustrated in FIG. **8** is approximately 7 degrees, though the angle of attack α could be less than or greater than that illustrative value. The angle of attack a can be introduced for either a right circular or an isentropic cone **70**. Positioning the cone at an angle of attack α with respect to the plane of particle release **63** results in a compression surface **72** with increased ability to diver boundary layer air as compared to a compression surface **72** formed from a cone not positioned at an angle of attack α with respect to the flow field.

FIG. **9A** shows an isentropic cone **70** CFD solution for a compression surface **72**. Through the procedures described above, the isentropic cone **70** will allow a CFD solution of the shape of an isentropic compression surface **72** of a different shape than the compression surface created by a circular cone of a constant semi-vertex angle. When the CFD derived flow field contacts the isentropic cone **70** shown in FIG. **9A**, it produces a conical shock **62** and an infinite number of weak shocks **90** that form an isentropic compression fan **91**. The isentropic compression fan **91** compresses to a focal point **92**, after which the conical shock **62** returns to a single shock state.

An isentropic compression surface **72** provides technical advantages over a compression surface created from a constant vertex right circular cone. The isentropic compression surface **72** allows the utilization of a smaller inlet capture area to reduce weight and aid integration onto the aircraft. Furthermore, designing the isentropic compression surface **72** from an isentropic cone **70** that produces a focal point **92** outside the cowl **30** will allow for better performance because the air flows through a series of weak shock waves **90** rather than merely one strong conical shock wave and a terminal shock wave. A bump **20** with a compression surface **72** shaped based on an isentropic cone **70** with an initial deflection angle of 12° and a final deflection angle of 21°, for example, will produce an isentropic compression fan **91** with a focal point **92** outside the cowl **30**.

FIG. **9B** shows the integration of one embodiment of an isentropic bump **20** with the forward-swept aft-closing cowl **30** that includes an isentropic compression surface **72** created from an isentropic cone **70** positioned at an angle of attack α. The compression surface **72** in this embodiment has all of the advantages of a compression surface **72** formed without an angle of attack, with the additional advantage that the isentropic bump **20** of FIG. **9B** can have an increased performance in diverting boundary layer air relative to an isentropic bump **20** with a compression surface **72** formed from an isentropic cone **70** without an angle of attack α.

FIG. **9B** shows a cut-away side view of the bump **20** comprising a compression surface **72**, a transition shoulder **73**, and a diffuser fairing **74**. The compression surface **72** terminates at the k/w point within the inlet. The transition shoulder **73** begins at the termination of the compression surface **72**. In the embodiment described in FIG. **9B**; the surface of the transition shoulder **73** initially has an angle in relation to the body of the aircraft approximately equal to the total turning angle of the compression surface **72**. This angle gradually decreases until the angle of the surface of the transition shoulder **73** in relation to the body of the aircraft approaches approximately zero so the surface of the transition shoulder **73** is approximately parallel to the body of the aircraft, at which point the transition shoulder **73** terminates. The termination point of the transition shoulder **73** (when the angle of the surface of the transition shoulder **73** in relation to the aircraft body is approximately zero) defines the minimum throat area **76**, or minimum flow area, of the inlet. A diffuser fairing **74** begins at the termination of the transition shoulder **73**. The diffuser fairing **74** can gradually decrease in the height the surface of the bump **20** is raised away from the body of the aircraft body as the diffuser fairing **74** continues toward the aft of the inlet.

FIGS. **10A** and **10B** show graphical representations of the compression surface **72** and the transition shoulder **73**. While both figures represent a compression surface derived as outlined above, FIG. **10 2** represents an embodiment of the transition shoulder **73** with improved boundary layer diversion.

The graphs in FIGS. **10A** and **10B** plot the surface slope in degrees on the y axis versus the bump station in inches (moving forward to aft) on the x axis. The different lines of plotted data on each graph indicate the surface slope versus the bump station at various radial locations on the surface of the bump **20**. The inset indicates how to determine the radial location, described by the angle ϕ with relation to the bump centerline. For example, when the angle ϕ is zero degrees, this radial location represents approximately the plane of symmetry for the inlet (for example, the line represents the plot for a radial location described when ϕ is approximately zero degrees). The angle ϕ increases as the radial location on the surface of the bump **20** moves outboard. The solid vertical line in the graph represents the point where the compression surface terminates and the transition shoulder begins; thus, the portion of the graph to the left of the solid line represents the compression surface **72** and the portion to the right represents the transition shoulder **73**.

The compression surface **72** geometry is identical on both FIGS. **10A** and **10B** and is defined by the CFD analysis described earlier. In both FIGS., the dashed line, shown in the legend representing a ϕ of approximately 0°, shows a surface slope of approximately 19.5° at the termination of the compression surface **72**; the dash, two dot, dash line, representing a ϕ of approximately 40°, shows a surface slope of approximately 14° at the termination of the compression surface **72**. These FIGUREs illustrate that as the radial location moves outboard, the peak angle at that bump station declines. In FIG. **10A**, the slope of the surface reaches a maximum for each radial location of the bump at the point where the compression surface terminates and the transition shoulder begins, or at approximately forty-one inches for the embodiment of FIG. **10A**. The reduction in slope from the beginning of the transition shoulder at approximately forty-one inches to the end of the transition shoulder at approximately sixty-seven inches is constant. Each of the curves is a straight line, representing a pure radius of curvature having a constant turn rate, from the maximum surface slope at the termination of the compression surface **72** to a zero surface slope at the termination of the transition shoulder **73**. Thus, for the transition shoulder described in FIG. **10**A, the change in degrees per inch is approximately a constant for each radial location. In FIG. **10**B, represents a different shape of the transition shoulder **74**. In FIG. **10**B, the slope of the surface reaches a maximum at a different bump station location for each different radial location. For example, while the dashed line for a ϕ of approximately 0° still shows a peak surface slope (of approximately 19.5°) at the termination of the compression surface **72**, the dash-two dot-dash line for ϕ of approximately 40° shows a peak surface slope of approximately 19.5° at a bump station well into the transition shoulder **73** portion of the bump **20** (at approximately 50 inches) Thus, rather than having reduction in surface slope for all radial locations beginning at the termination of the compression surface, the peak surface slope occurs increasing further into the transition shoulder **73** until a radial location of approximately 60°. Rather than a straight line from the point where each radial cut intersects the termination of the compression surface to the termination of the transition shoulder (as in FIG. **10**A), a significant number of the radial cut plots rise to a nearly equivalent peak surface slope before falling back to zero. For example, the dash-two dot-dash line for the radial location of approximately 40° intersects the vertical separation line in FIG. **10**B at approximately 14°. However, instead of dropping immediately down to 0°, the dash-two dot-dash line increases again from 14° to approximately 19°, where it then drops down to 0° at a bump station of approximately sixty-six inches. These FIGUREs illustrate that while the slope of the dashed line for ϕ of approximately 0° in FIG. **10**A has the highest slope, the slope of the dashed line for ϕ of approximately 0° in FIG. **10**B has a lower slope than a significant number of the other plotted lines. Controlling the slopes of the lines after the termination of the compression surface **72** determines the shape of the transition shoulder **73**.

In operation, the embodiment of the transition shoulder **73** in FIG. **10**B provides a technical advantage over the embodiment of the transition shoulder **73** of FIG. **10**A by increasing the amount of boundary layer air that will be diverted outboard. The amount of boundary layer air diverted outboard increases because this embodiment of the transition shoulder **73** of FIG. **10**B creates a greater spanwise static pressure gradient than the transition shoulder **73** embodiment of FIG. **10**A.

FIG. **11** shows the design parameters for determining a transition shoulder with a varying rate of surface slope change relative to radial location. As shown in the front view legend in FIG. **11**, the radial location on the surface of the transition shoulder is zero degrees along the centerline of the transition shoulder. The radial location value in degrees increases as radial location moves outwardly away from the centerline of the transition shoulder.

FIG. **11** the bump **20** has a transition shoulder **73** beginning at the Bstop station **110** and terminating at the throat station **111**. The surface **112** of the transition shoulder **73** shown in FIG. **11** consists of two surface portions along surface **112**, the first defined by the length L_1 from the Bstop station **110** to the intersection of the transition shoulder **113**, and the second defined by L_2 from the intersection **113** to the throat station **112**. The shape of the surface portion **111** of the transition shoulder **73** is defined by the radius R_1 for the length L_1 and by the radius R_2 over the length L_2, where the radii R_1 and R_2 are defined by the following formulas:

$$R_1 = \frac{L_1/2}{\mathrm{Sin}\left(\frac{\theta_2 - \theta_1}{2}\right)\mathrm{Cos}\left(\frac{\theta_2 + \theta_1}{2}\right)}$$

$$R_2 = L_2/\mathrm{Sin}(\theta_2)$$

where

θ_1=Surface Slope Angle at Bstop Station

θ_2=Maximum Surface Slope Angle

$$L_1 + L_2 = F.\ S.)_{Throat} - F.\ S.)_{Bstop}$$

$$0 \leqq L_2 \leqq F.\ S.)_{Throat} - F.\ S.)_{Bstop}$$

$$L_2 \equiv \theta_2/1.5 @ \phi = 55°$$

As shown in FIG. **11**, the shape of the first surface portion is concave and is formed according to the arc defined by R_1 rotated about a point on the Bstop station away from the body of the aircraft. The shape of the second surface portion is convex and is formed according to the arc defined by R_2 rotated about a point on the throat station toward the body of the aircraft.

In the above equations, $F.\ S.)_{Throat}$ and $F.\ S.)_{Bstop}$ represent fuselage stations on the surface of the aircraft. For a typical aircraft application, bump station of zero inches can correspond to a fuselage station of approximately 262.3 inches. $F.\ S.)_{BSTOP}$ represents the point at which the compression surface **72** ends and transition shoulder **73** begins. $F.\ S.)_{Throat}$ represents the point at which the transition shoulder **73** terminates. The throat station point is a function of the length of the aircraft and the Bstop station is a user defined point. L_1+L_2 is a constant distance defined by the difference between $F.\ S.)_{Throat}$ and $F.\ S.)_{BSTOP}$. While L_1+L_2 is always constant, each surface portion length varies depending on radial location. For example, L_1 at ϕ=40 degrees can be longer than L_1 at ϕ=0 degrees.

The maximum surface slope angle (θ_2) is a constant (for the embodiment illustrated in FIG. **10**B, θ_2 equals approximately 19.5°) that is defined at the Bstop station for a radial location of zero degrees. While other radial locations may have different bump stations at which the maximum surface slope angle occurs, the surface slope angle will never exceed the surface slope angle at the Bstop station for a radial location of zero degrees.

The surface slope angle at Bstop Station (θ_1) is a known value that changes based on the radial location. In FIG. **10**B, a radial location of 0° the surface slope angle is approximately 19.5°; for a radial location of 10° the surface slope angle is approximately 18°; and so forth.

At the Bstop station, L_2 is defined to be zero. L_2 is then determined for a radial location ϕ of 55° according to the above equation ($L_2=\phi_2/1.5@\phi=55°$) The 1.5 factor was determined through analysis as a constant whose use would result in an improved transition shoulder. Other factors could possibly be used in this equation. By assuming a linear regression between the points defining $L_2@\phi=0°$ and $L_2@\phi=55°$ with a straight line, L_2 can be determined for radial locations between zero and fifty-five degrees. For the embodiment of FIGS. **10**B and **11**, L_2 values were determined for radial locations of **10**, **20**, **30**, **40**, and 50 degrees. While the embodiment described by FIGS. **10**B and **11** use a straight line regression to determine L_2 for radial locations up to 55°, other regression analyses could also be used to determine L_2. For radial locations exceeding 55°, the user defines L_2. FIG. **10**B shows one example of how to define **81** and $\mathbf{74}_2$ at radial locations in excess of 55°. The values of L_1at equivalent radial locations can then be determined from the L_2 values (by subtracting L_2 from the total distance from Bstop to throat station). Once θ_2, θ_1, L_1 and L_2 have been determined for each radial location ϕ, R_1 and R_2 can be calculated for each radial location ϕ using the equations for R_1 and R_2 stated earlier.

As shown in FIG. **11**, the slope of the surface of the transition shoulder **73** will increase from the Bstop station **110** over the length L_1 to a maximum slope at the intersection **113**, and will then decrease over the length L_2 to a slope of zero at the throat station **112**. Thus, the graphical representation of the transition shoulder surface slope of FIG. **10B** shows that the intersection **113** for the transition shoulder represented in FIG. **10B** occurs at a bump station of approximately 50 inches for a radial location of 40 degrees. As FIG. **10B** illustrates, the maximum surface slope of the transition shoulder **73** will occur at different bump stations for different radial locations ϕ FIG. **12** shows an isometric view of the compression surface **72** and transition shoulder **73** graphically represented in FIG. **10B**. As shown in FIG. **12**, the maximum or peak surface slope occurs at varying distances aft of the initiation of the compression surface **120**. This varying aft distance is illustrated by the line depicting the locus of peak surface slope **120**. This also indicates that L_1 and L_2 will vary as the radial location ϕ varies.

FIG. **13** illustrates improved boundary layer diversion of the present invention using a compression surface designed from an isentropic cone with a seven degree angle of attack and a transition shoulder with a varying rate of decrease in surface slope (illustrated as Design B) as compared to the boundary layer diversion of an embodiment of the present invention using a compression surface designed with no angle of attack and with a transition shoulder with a constant rate of change in surface slope (illustrated as Design A). Design B of FIG. **13** shows the particle trace paths **50** of the boundary layer air pushed further outboard as compared to the particle trace paths **50** of the boundary layer air associated with the embodiment of Design A. The CFD analysis performed on these two embodiments indicate approximately 1% improvement in total performance for Design B over Design A.

In summary, the present invention provides a diverterless engine inlet system that utilizes a bump with an isentropic compression surface, a transition shoulder and a diffuser fairing in combination with an aft-closing forward-swept cowl to divert boundary layer air from an aircraft engine inlet. The present invention eliminates the need for a boundary layer diverter, an overboard bypass system, and a boundary layer bleed system currently used on conventional air induction systems for supersonic aircraft. The present invention reduces aircraft weight, cost, and complexity. These features are eliminated because the compression surface and cowl work synergistically to provide a passive boundary layer diversion capability.

Although the present invention has been described in detail, it should be understood that various changes, substitutions and alterations can be made hereto without departing from the spirit and scope of the invention as described by the appended claims.

What is claimed is:

1. A system for diverting boundary layer air from an aircraft engine inlet, comprising:

a surface raised outwardly from the body of the aircraft, said surface comprising;

a compression surface near the opening of said inlet;

a diffuser fairing; and

a transition shoulder beginning at the Bstop station and ending at the throat station, said transition shoulder having a varying rate of change of surface slope relative to radial location on the surface of said transition shoulder, said transition shoulder operable to create a greater spanwise static pressure gradient to increase the amount of boundary layer air diverted from the aircraft inlet.

2. The system of claim **1** wherein the radial location on the surface of said transition shoulder is zero degrees along the centerline of the transition shoulder and increases as the radial location moves outwardly away from the centerline of the transition shoulder.

3. The system of claim **2** wherein the transition shoulder surface further comprises a first surface portion of length L_1 and a second surface portion of length L_2, said first surface portion defined by an arc according to a first radius R_1 and said second surface portion defined by an arc according to a second radius R_2.

4. The system of claim **3** wherein said arc according to R_1 is defined by R_1 centered on the Bstop station and rotated to form a concave first surface portion, and further wherein said arc according to R_2 is defined by R_2 centered on the throat station rotated to form a convex second surface portion.

5. The system of claim **4** wherein the first surface portion has a varying length L_1 depending on radial location and the second surface portion has a varying length L_2depending on radial location, and further wherein the sum in length of L_1 and L_2 equals the distance between the Bstop station and the throat station.

6. The system of claim **5** wherein the maximum surface slope angle θ_2 at any point along the surface of the transition shoulder is a constant and is determined at the Bstop location for a radial location of zero degrees.

7. The system of claim **6** wherein the Bstop station surface slope angle θ_1 is a maximum at a radial location of zero degrees and gradually decreases for increasing radial locations.

8. The system of claim **7** where first radius R_1, second radius R_2 are defined by the formulas:

$$R_1 = \frac{L_1/2}{\mathrm{Sin}\left(\frac{\theta_2-\theta_1}{2}\right)\mathrm{Cos}\left(\frac{\theta_2+\theta_1}{2}\right)}$$

$$R_2 = L_2/\mathrm{Sin}(\theta_2)$$

9. The system of claim **8** wherein for a radial location of zero degrees L_2 =0.

10. The system of claim **9** wherein for a radial location of 55 degrees, the second length L_2 is defined by the following equation:

$$L_2 \equiv \theta_2/1.5\ @\phi=55°$$

11. The system of claim **10** wherein the second length $L_2$for any other radial location is determined through a linear regression analysis between L_2at zero degrees and L_2 at fifty five degrees.

12. The system of claim **10** wherein the second length L_2 is defined by the following equation:

$$L_2\theta_2/X @\phi=55°$$

where X is a numeric value greater than 1.5.

13. The system of claim **10** wherein the second length L_2 is defined by the following equation:

$$L_2 \equiv \theta_2/X @\phi=55°$$

where X is a numeric value less than 1.5.

14. A method for diverting boundary layer air from an inlet comprising;

forming a compression surface raised outwardly from the body of the aircraft in the boundary layer air path to initially alter the flow of the boundary layer air;

forming a transition shoulder beginning at the Bstop station, delineating the termination of the formed compression surface, and ending at the throat station, said transition shoulder having a surface wherein the radial location on the surface of said transition shoulder is zero degrees along the centerline of the transition shoulder and increases as the radial location moves outwardly away from the centerline of the transition shoulder;

varying the rate of change of surface slope relative to radial location on the transition shoulder surface, thereby increasing the spanwise static pressure gradient to further divert boundary layer air; and

diverting substantially all of said boundary layer air to prevent said boundary layer from entering said inlet.

15. The method of claim 14 wherein forming a transition shoulder further comprises forming the transition shoulder surface with a first surface portion of length L_1 and a second surface portion of length L_2.

16. The method of claim 15 further comprising defining the shape of said first surface portion by an arc according to a first radius R_1 and defining the shape of said second surface portion by an arc according to a second radius R_2.

17. The method of claim 16 wherein said defining the shape of said first surface portion further comprises centering R_1 on the Bstop station and rotating R_1 to form a concave first surface portion, and wherein defining the shape of said second surface portion further comprises centering R_2 on the throat station and rotating R_2 to form a convex second surface portion.

18. The method of claim 17 further comprising;

varying the length L_1 of the first surface portion according to radial location;

varying the length L_2 of the second surface portion according to radial location; and

maintaining the sum in length of L_1 and L_2 at any radial location equal to the distance between the Bstop station and the throat station.

19. The method of claim 18 further comprising determining a maximum surface slope angle θ_2 at the Bstop station for a radial location of zero degrees, and maintaining that maximum surface slope angle at any point along the surface of the transition shoulder.

20. The method of claim 19 further comprising forcing the maximum surface slope angle θ_1 at the Bstop station to occur at a radial location of zero degrees, and gradually reducing the surface slope angle at the Bstop station for increasing radial locations.

21. The method of claim 20 further comprising defining first radius R_1 and second radius R_2 by the formulas:

$$R_1 = \frac{L_1/2}{\text{Sin}\left(\frac{\theta_2-\theta_1}{2}\right)\text{Cos}\left(\frac{\theta_2+\theta_1}{2}\right)}$$

$$R_2 = L_2/\text{Sin}(\theta_2)$$

22. The method of claim 21 further comprising setting the value of L_2 =0 at a radial location of zero degrees.

23. The method of claim 22 further comprising defining the value of the second length L_2 for a radial location of fifty-five degrees by the following equation:

$$L_2 \equiv \theta_2/1.5 \ @\phi=55°$$

24. The method of claim 23 further comprising determining the value of second length L_2 for any radial location other than zero and fifty-five degrees by performing a linear regression analysis between L_2at zero degrees and L_2at fifty five degrees.

25. The method of claim 24 further comprising defining the value of the second length L_2 at a radial location of fifty-five degrees by the following equation.

$$L_2 \equiv \theta_2 /X @\phi=55°$$

where X is a numeric value greater than 1.5.

26. The method of claim 24 further comprising defining the value f the second length L_2 at a radial location of fifty-five degrees by the following equation:

$$L_2 \equiv \theta_2 /X @\phi=55°$$

where X is a numeric value less than 1.5.

27. A method for determining the shape of a varying slope transition shoulder to use in a system for diverting boundary layer air from an inlet comprising the steps of:

determining the length of a transition shoulder beginning at a Bstop station and terminating at a throat station, said transition shoulder surface length comprising the sum of the first surface portion length L_1 and a second surface portion length L_2;

defining the maximum surface slope θ_2 as the surface slope at the Bstop station for a radial location of zero degrees;

defining L_2 equal to zero for a transition shoulder surface radial location of zero degrees;

defining L_2equal to θ_2/X for a transition shoulder surface radial location of fifty-five degrees, where x is a constant value between 1 and 10;

performing a regression analysis to determine the value of L_2 for a plurality of radial locations between zero and fifty-five degrees;

determining the values of L_1 at the plurality of radial locations between zero and fifty-five degrees from the corresponding values of L_2;

determining a first radius R_1 and second radius R_2 by the formulas:

$$R_1 = \frac{L_1/2}{\text{Sin}\left(\frac{\theta_2-\theta_1}{2}\right)\text{Cos}\left(\frac{\theta_2+\theta_1}{2}\right)}$$

$$R_2 = L_2/\text{Sin}(\theta_2)$$

defining the transition shoulder first surface portion of length L_1 to have a concave contour according to said first radius R_1; and

defining the shape of transition shoulder second surface portion of length L_2 to have a convex contour according to said second radius R_2.

28. The method of claim 27 further comprising applying the transition shoulder to a surface of an aircraft as part of a boundary layer diversion system.

* * * * *